The Sumatra-Andaman Tsunami in Banda Aceh: A Linear Model for Representation

O Tsunami de Sumatra-Andaman em Banda Aceh: Um Modelo Linear para Representação

El Tsunami de Sumatra-Andaman en Banda Aceh: Un Modelo Lineal para la Representación

Jorge Corrêa de Araújo[1]
State University of Rio de Janeiro (UERJ), São Gonçalo, RJ, Brazil
https://orcid.org/0000-0002-1015-6311, http://lattes.cnpq.br/3486694358849656

Rosa García Márquez[2]
State University of Rio de Janeiro (UERJ), São Gonçalo, RJ, Brazil
https://orcid.org/0000-0003-3465-569X, http://lattes.cnpq.br/1466957291722861

Abstract: The Sumatra-Andaman earthquake that occurred on December 26, 2004 was the second largest earthquake in the past 40 years, with a moment magnitude of $9.1 - 9.3$. The rupture took place at a depth of $1.3\ km$ along a large boundary fault between the Indian and Burma plates. The fault slip reached up to 20 meters near Banda Aceh, Sumatra Island, and was more rapid compared to the northern end between the Indian Plate and the Andaman archipelago, where landslide took almost one hour to reach from 7 to 20 meters. Based on this data and other observations, it was possible to estimate that the main tsunami originated approximately $390\ km$ from Banda Aceh city. Although the energy transmitted by the simple harmonic waves adopted in this study was shorter than that reported by other references, it was still significant. The estimated arrival time for the tsunami in Banda Aceh using a simple model was reasonably consistent with the actual observation time. This agreement suggests that the origin region of the estimated in this study is likely within the most probable starting point of the tsunami. The wave amplitude near the coast, as estimated by the model, fell within the observed range reported by the references. The methodology developed in this study seems to be suitable for obtaining initial estimates of several important parameters involved in events of this nature.

Keywords: wave speed; wave energy; linear model.

Resumo: O terremoto de Sumatra-Andaman que ocorreu em 26 de dezembro de 2004 foi o segundo maior terremoto dos últimos 40 anos, com uma magnitude de momento entre $9,1$ e $9,3$. A ruptura ocorreu a uma profundidade de $1,3\ km$ ao longo de uma grande falha de fronteira entre as placas Indiana e de Burma. O deslizamento da falha atingiu até 20 metros perto de Banda Aceh, na ilha de Sumatra, e foi mais rápido em

[1] **Brief curriculum**: PhD in Computational Modeling from the Polytechnic Institute of the State of Rio de Janeiro and associate professor at the State University of Rio de Janeiro (UERJ), São Gonçalo, RJ, Brazil. **Authorship contribution**: Conceptualization, formal analysis, writing – original draft. **Contact**: jorgecorreadearaujo55@gmail.com.

[2] **Brief curriculum**: PhD in Mechanical Engineering from the Federal University of Rio de Janeiro (UFRJ) and associate professor at the State University of Rio de Janeiro (UERJ), São Gonçalo, RJ, Brazil. **Authorship contribution**: Writing – review and editin. **Contact**: rosagmarquez@yahoo.com.br.

comparação com a extremidade norte entre a placa Indiana e o arquipélago de Andaman, onde o deslizamento levou quase uma hora para atingir de 7 a $20\ m$. Com base nesses dados e outras observações, foi possível estimar que o principal tsunami teve sua origem a aproximadamente $390\ km$ da cidade de Banda Aceh. Embora a energia transmitida pelas ondas harmônicas simples adotadas neste estudo tenha sido menor do que a relatada por outras referências, ainda assim, ela foi significativa. O tempo estimado de chegada do tsunami em Banda Aceh usando o modelo simples foi razoavelmente consistente com o tempo de observação real. Entre os tempos de chegada da onda sugere que a região de origem da onda estimada nesse estudo parece estar próxima da região onde efetivamente o fenômeno ocorreu. A amplitude da onda próxima à costa, conforme estimada pelo modelo, ficou dentro da faixa observada relatada pelas referências. A metodologia aqui desenvolvida parece ser adequada para obter estimativas iniciais de vários parâmetros de importância em eventos dessa natureza.

Palavras-chave: velocidade de onda; energia de onda; modelo linear.

Resumen: El terremoto de Sumatra-Andamán del 26 de diciembre de 2004 fue el segundo más grande de los últimos 40 años, con una magnitud de momento entre 9.1 e 9.3. La ruptura ocurrió a una profundidad de $1.3\ km$ a lo largo de una gran porción do límite de la falla entre las placas indiana y birmana. Cerca de Banda Aceh, en la isla de Sumatra, se produjo un deslizamiento de falla de hasta 20 metros, que fue más rápido en comparación con el extremo norte entre la placa indiana y el archipiélago de Andamán, donde el deslizamiento tomó casi una hora para deslizar 7 a $20\ m$. Con estos datos y otras observaciones, pudimos estimar que el principal tsunami tuvo su a aproximadamente $390\ km$ de la ciudad de Banda Aceh. A pesar de que a energía transmitida por las ondas armónicas simples adoptadas en este estudio fue más corta que la informada por las otras referencias, todavía así, ella es significativa. El tiempo estimado de llegada del tsunami a Banda Aceh utilizando el modelo simple fue razonablemente consistente con el tiempo de observación real. El tiempo de llegada de la onda sugiere que la región de origen de la onda estimada en este estudio parece estar próxima de la región principal donde ocurrió el fenómeno. La amplitud de la onda cerca de la costa, estimada por el modelo, se encontraba dentro de la faja observada por las referencias. La metodología aquí desarrollada parece ser adecuada para obtener estimaciones iniciales sobre varios parámetros de importancia en eventos de esta naturaleza.

Palabras clave: velocidad de onda; energía de las olas; modelo lineal.

Submitted: March 30, 2023.

Approved: July 25, 2023.

1 Introduction

The Sumatra-Andaman earthquake on 26 December 2004 was the second largest earthquake in the instrumental record and the third most fatal. This earthquake had moment magnitude, $M_w = 9.3$ with its energy release $E_R = 4.3 \times 10^{18}(J)$ equivalent to a 100-gigaton bomb, according to Bilham [2] or $E_R = 1.1 \times 10^{18}(J)$ second Lay *et al*. [11]. As reported by Lay *et al*. [11], unfortunately the accurate E_R estimation, especially for great earthquakes with long sources duration, is difficult. The primary shock involving the plates of India and Burma gave rise to tsunamis ("waves in the harbor") that propagated at great speed through the Indian Ocean reaching several countries in that region, notably the province of Aceh on the island of Sumatra in Indonesia, with the first wave arriving about 40 minutes after the main shock. In Sri-Lanka as reported by Santos [14], the tsunami arrived two hours later while in the cities of Vishakapatnan and Chenay at east coast of India in Tami Nadu region, the wave arrived about $157\ min$ later, see Lay *et al*. [11]. Within minutes after the earthquake at $3.3^oN, 96^oE$, at a depth of about $30\ km$, at $00:58:53\ GMT$ a powerful tsunami struck the coast near the northwestern tip of Sumatra especially Banda Aceh, the largest city of the region, where wave heights of $5-12\ m$ were reported by Shearer and Burgmann [15] and more than $100,000$ people were killed. The Figure 1 shows schematically the rupture zone of approximately divided in three segments, begging southeast of Sumatra and expanded for the central and northern parts.

Figure 1 – Rupture front direction along the segments of Sumatra, Nicobar and Andaman in the firstly $600s$ after the epicenter located at 3.3^oN96^oE

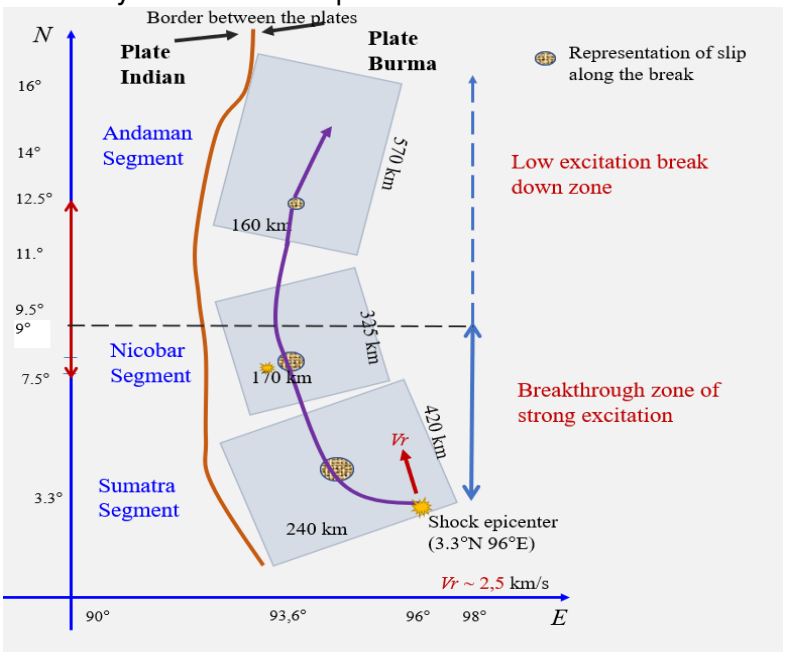

Source: Based in Figure 8 of Lay *et al*. [11].

As reported by Santos [14], the Indian plate shifts (*slip*) under of the Burma plate in a known process as subduction, what provoked a mean vertical elevation of the sea floor (*uplift*) about $4\ m$ for the southern half of the fault line and about $2\ m$ northern half geological faults. As reported by Lay *et al*. [11], the western margins of the Andaman and Nicobar Islands were uplifted with the eastern margins being submerged (subsidence) and this can be accounted for by the substantial slip of about $10\ m$ on a $160\ km$ wide thrust plane in the northern half of the rupture zone or by less slip on more steeply dipping splay faults. In fact, post-seismic photographs obtained by Denis Giles showed in according with Bilham [2] that Nicobar Islands approximate 7^oN have sunk $2-4\ m$. The North Sentinel Island in the west of Nicobar segment had a uplift estimated to be $1-2\ m$, with the surrounding coral lagoon completely raised above the sea level after the earthquake. In the Indira Point lighthouse $(45.2'N, 93^o49.6'E)$ at east of Nicobar segment had a subsidence estimated to be $4.25\ m$ based on its foundation being $3.5\ m$ above sea level when constructed and now submerged $1.5m$ at high tide Bilham [2]. As reported by Lay *et al*. [11], the source region for strong initial tsunami excitation extends $600-800\ km$ north of the epicenter, terminating near the Nicobar Islands. Still second these authors, the northern third of the aftershock zone appears not to have produced rapid vertical ocean-bottom displacement capable of the generation large tsunami waves.

In fact, Bilham [2] affirmed that the slip in Andaman Islands (10^o-14^oN) was development slowly, what could prevent a strong tsunami in this region. Bilham [2] gave especial attemption on the reverse slip occurred in the central and northern parts of the rupture zone between $600-1300km$ from the epicentre, particularly the observed synthetic deformations in the Nicobar segment at 7.5 ± 1^oN and Andaman segment at 12.5 ± 1^oN, where are showed subsidence from to $4\ m$ distributed along $150\ km$ for east and uplift from $7\ m$ to east. Of the various articles referenced in this work on the Sumatra-Andaman earthquake in 2004, most authors deal with the phenomenon eminently from the view point of seismological research, leaving only Santos [14] to disclose some data on the wavelength of wave water, the average depth of the Indian Ocean, the wave speed, the mechanical energy of the tsunami and the time of rupture or propagation of the main shock. However this author used basic elementary physic formulas and other simplifications that gave origin some distorted results as by example, the vertical displacement of water in the seafloor volume V approximate $3.9\times10^{11}\ m^3$ largest longer than the reported by Bilham [2] as volume greater than $30\ km^3$. Bilham [2] does not show how obtained these estimates.

Our aim is to present, in a succinct manner, the linear theory of small amplitude water wave motion as a representational model for the 2004 Sumatra-Andaman tsunami that targeted Banda

Aceh coast on the Island of Sumatra. Estimate the likely location of the main principal tsunami formation, its energy and arriving time wich the first wave reached the coast of Banda Aceh using a linear simple model to describe these phenomenon.

2 Methods

In this section, the formulation of the general surface wave problem and the cubic splines are given.

2.1 Formulation of the general surface wave problem

The Figure 2 shows a schematic representation for a surface wave problem like that on any ocean beach. The water is assumed to be initially at rest and to fill the space $D \subset \mathbb{R}^3$ defined by $-d(x,y) \leq z \leq 0, -\infty < y < \infty$, $x \geq 0$, where z is the distance between the bottom and the water assumed at rest, y represents a quantity of length and x is the direction of motion. At the time $t = 0$, a disturbance is created on the surface of the water over the D region, and a subsequent motion of the water can be occurs. In Figure 2, $\vec{V} = u\vec{i} + v\vec{j} + w\vec{k}$ is the velocity field for the water motion, where u, v and w are functions of $x, y, z; t$ and are the velocity components in the respectively x, y and z directions while $z = \eta(x, y; t)$ represents the S free surface of the wave.

Figure 2 – A general surface water wave problem

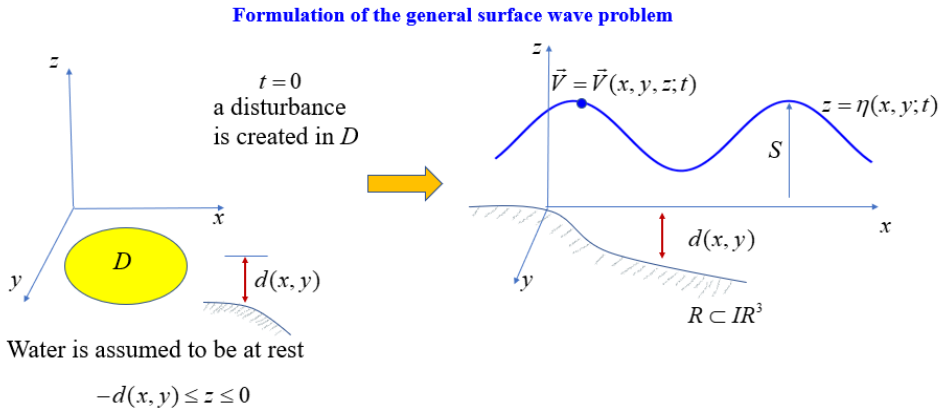

Source: Authors' elaboration.

In this form, the determination of the velocity distribution in the region occupied by the fluid no attemption is gave to follow the motion of individual particles, but rather observing the velocity distribution at fixed points in space as a function of the time, in an Eulerian form Stoker [16]. To simplify the mathematical analysis it's assumed that the fluid motion is irrotacional. In accordance with Dean and Dalrymple [4], this is because the viscous effects are usually concentrated in thin boundary layers near the surface and the bottom. Besides then was assumed that is incompressible, *i.e.*, constant density. With this assumption a velocity potential, $\psi = \psi(x, y, z; t)$ exists, $\vec{V} = -\psi$. The Euler equations that represented the motion of waves are given by Fox *et al*. [6]

$$\frac{D\vec{V}}{Dt} = -\frac{1}{\rho}\nabla p - g\vec{k}, \tag{1}$$

where ρ is the density of the fluid (water), p is the hydrostatic pressure and g the gravity force in z direction. This equation can be written as the Navier-Stokes equations making the viscosity equal zero to obtain by Debnath and Bhatta [5]

$$\frac{\partial\vec{V}}{\partial t} + (\vec{V}\cdot\nabla)\vec{V} = -\frac{1}{\rho}\nabla p - g\vec{k}, \tag{2}$$

where

$$\vec{V}\cdot\nabla \equiv (u, v, w)\cdot\left(\frac{\partial}{\partial x}, \frac{\partial}{\partial y}, \frac{\partial}{\partial z}\right)^t. \tag{3}$$

Since the mass flux through any fixed closed surface enclosing a region $3 - D$ in which no liquid is created or destroyed is zero, we have the equation

$$\iint_S \rho v_n dS = 0, \tag{4}$$

where $v_n = \vec{V}\cdot\vec{n}$ is the velocity component taken positive in the direction of the outward normal to the S surface. As the fluid is incomprehensible and using the Gauss's divergence theorem [8], results

$$div\vec{V} = u_x + v_y + w_z = 0. \tag{5}$$

This equation is called equation of continuity or mass conservation. Since $\vec{V}$ has a velocity potential we obtained from equation (5)

$$\nabla^2\psi = \psi_{xx} + \psi_{yy} + \psi_{zz} = 0. \tag{6}$$

So ψ must satisfy the Laplace equation, i.e, ψ is a harmonic function. This fact represents an important simplification because requires that the scalar function ψ satisfy a linear partial differential equation (PDE) that is easier treatment. To simplify the mathematical analysis, will be adopted the

2-D dimension and other assumptions involving the region of interest basing the treatment in the description realized by Dean and Dalrymple [4] for the two-dimensional periodic water wave boundary value problem. The Figure 3 shows the fluid domain of one wave and the boundary conditions, where H is the height of the wave while $a = H/2$ is its amplitude.

Figure 3 – A particular boundary value problem for periodic water waves

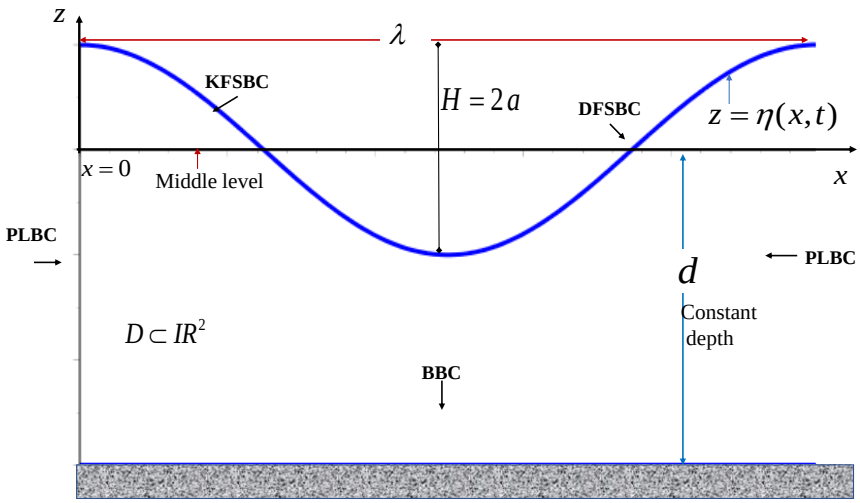

Source: Authors' elaboration.

The Laplace equation must be assured for the D domain, *i.e.*,

$$\nabla^2\psi = 0, \quad D: \ 0 < x < L, \ -d < z < \eta = \eta(x,t), \tag{7}$$

and

$$BBC: \ \frac{\partial\psi}{\partial z} = 0 \ \text{ or } w = 0, \quad z = -d, \tag{8}$$

$$DFSBC: \ \left(g\eta - \frac{\partial\psi}{\partial t}\right)_{z=0} = 0, \tag{9}$$

$$KFSBC: \ -\left(\frac{\partial\psi}{\partial z}\right)_{z=0} = \frac{\partial\eta}{\partial t}, \tag{10}$$

$$PLBC: \ \psi(x,t) = \psi(x+L,t), \tag{11}$$

$$PLBC: \ \psi(x,t) = \psi(x,t+T). \tag{12}$$

The BBC is the boundary bottom condition and is established that there is no flux of fluid through its or the vertical velocity is zero. The DFSBC is the dynamic free surface boundary condition and is obtained of the linearized Bernoulli law with $p = 0$ on free surface, $z = \eta(x,t)$. This law is

derived of the Euler equations and of the irrotacional character of the flow Stoker [16]. The KFSBC is the kinematic free surface boundary condition already linearized and can be obtained by total differentiation $\frac{d\xi}{dt} = \vec{V} \cdot \nabla\xi + \frac{\partial \xi}{\partial t}$ of the surface equation $\xi(x, z, t) = z - \eta(x, t) = 0$. The equations (11) and (12) are the periodic lateral conditions applied in both space and time respectively. The linearized equations (9) and (10) were possible with the assumption that the velocity of the water particles, the free surface elevation $z = \eta(x, t)$ and their derivates are all small quantities by Stoker [16] given origin the theory of waves of small amplitude. The convenient method for solving this linear partial differential equation (6) is by the separation of variables that in, according with Dean and Dalrymple [4], the solution of the boundary value problem is given by

$$\psi(x,t) = \frac{H}{2}\frac{g}{\sigma}\frac{\cosh(kd+z)}{\cosh(kd)}\cos(kx)\sin(\sigma\, t), \tag{13}$$

and

$$\eta(x,t) = \frac{H}{2}\cos(kx)\cos(\sigma\, t), \tag{14}$$

where $\sigma = \frac{2\pi}{T}$, with σ being the angular frequency and T the period. The equation (14) shows this wave is stationary. As reported by Dean and Dalrymple [4], standing waves often occur when incoming waves are completely reflected by vertical walls. Of the equations (9), (13) and (14) results the important dispersion equation given by

$$\sigma^2 = gk\tanh(kd), \tag{15}$$

where $k = \frac{2\pi}{L}$ is the number of wave. Multiplying the equation (15) by the factor $\frac{1}{k^2}$ can be obtained the velocity of the wave propagation, C as

$$C = \sqrt{\frac{g}{\lambda}\tanh\left(\frac{2\pi d}{\lambda}\right)} \text{ or } C = \sqrt{gd}, \text{ if } \frac{d}{\lambda} < 0.05. \tag{16}$$

The solution for no stationary waves or progressive waves is given by Stoker [16]; as Tsunamis are in general caused by earthquake motions of the ocean boundaries, have longer than $100\ km$, and if $\lambda \gg d$ (shallow waves) its C velocity propagation can be estimated by the simplified equation (16) with error by about 6% if the wave length is ten times the depth, and by less than 2% if the wave length is twenty times the depth by Stoker [16]. The solution for no stationary waves or progressive waves is given by Stoker [16] as

$$\psi(x,t) = \frac{H}{2}\frac{g}{\sigma}\frac{\cosh(kh+z)}{\cosh kh}\sin(kx-\sigma t), \tag{17}$$

$$\eta(x,t) = \frac{H}{2}\cos(kx-\sigma t). \tag{18}$$

The energy over a wave length λ at any arbitrary fixed time is given by Stoker [16] and here written by 2-D dimension as

$$E_\lambda = \rho \int_{z=-d}^{\eta} \int_{x=0}^{\lambda} \left(\frac{\psi_x^2 + \psi_z^2}{2} + gz \right) dx\ dz\ \ (J). \tag{19}$$

$E_o = \rho \int_{-d}^{\eta} \int_0^{\lambda} z\, dx\ dz$ is the potential energy for the water of depth d when at rest. So using the equation (19) and E_o for 2-D dimension reported by Stoker [16] we have

$$E_\lambda - E_o = \rho \int_{-d}^{\eta} \int_0^{\lambda} \left(\frac{\psi_x^2 + \psi_z^2}{2} \right) dxdz + \rho \int_0^{\eta} \int_0^{\lambda} gz\, dxdz, \ \ \left(\frac{J}{m} \right). \tag{20}$$

Of the equation (20) can be obtained the average energy in the fluid per unit length in the x-direction which results from the motion given by Stoker [16]

$$E_{av} = \frac{E_\lambda - E_o}{\lambda}, \ \ \left(\frac{J}{m^2} \right). \tag{21}$$

In according to Dean and Dalrymple [4], the total average energy by unit surface area is given by

$$E_{av} = \frac{1}{8} \rho g H^2, \tag{22}$$

and the total energy per wave per unit width is then simply, according to Dean and Dalrymple [4]

$$E_\lambda = \frac{1}{8} \rho g H^2 \lambda. \tag{23}$$

Assumed energy conservation in this process and that the wave front extension remains unchanged, can be obtained the Green's Law [4]

$$\frac{H_2}{H_1} = \left(\frac{h_1}{h_2} \right)^{1/4}. \tag{24}$$

2.2 **Cubic Splines Interpolation**

As reported by Margaritondo [12] the change in speed with the depth has a fundamental implication on the height of the wave. So in equation (16) the speed decreases as the wave approaches of the shore with significant increase in height and therefore our simple model will have discontinuities when the wave passed from a place of greater depth to one of lesser depth as shown in Figure 4. The increase in height as the tsunami reaches a shore is due to the conservation of energy because the tsunami cause only a propagation pertubation of the local motion of water particles [12].

The profile of $z = \eta(x,t)$ changes with depth d and therefore this representation will have discontinuities as shown in Figure 4.

Figure 4 – The form of water wave changes with the depth

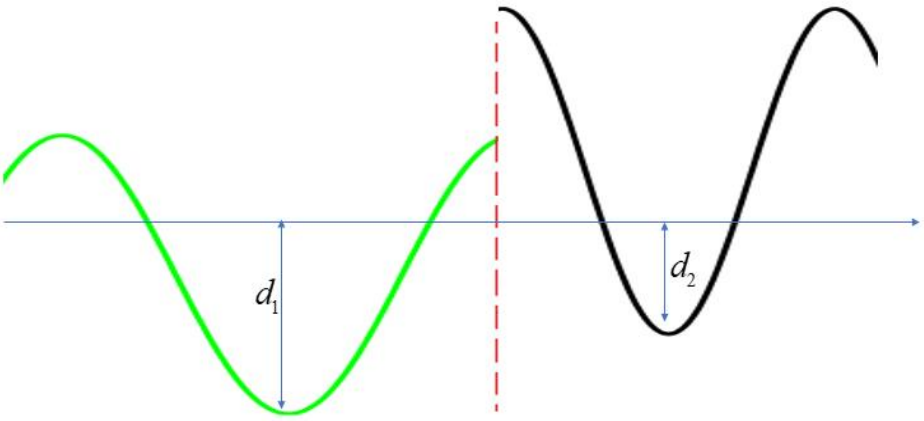

Source: Authors' elaboration.

The goal is, given a set of points, get an interpolating cubic polynomial where

$$S(x) = \begin{cases} y_1 = S_1(x), & x_1 \leq x \leq x_2 \\ y_2 = S_2(x), & x_2 \leq x \leq x_3 \\ \vdots & \\ y_{n-1} = S_{n-1}(x), & x_{n-1} \leq x \leq x_n \end{cases} \tag{25}$$

with $S_i(x), i = 1, ..., n-1$, being different cubic polynomials. The requirements are that $S(x)$, $S'(x)$ and $S''(x)$ must be continuous in $x_1 \leq x \leq x_n$ and $S^{(iv)}(x) = 0$. So the continuity condition of the $S''(x)$ creates a unique smooth curve going through these points while the fourth derivate of S equals zero stems from the linear theory of beams for small displacement. Therefore, when changing the depth of the ocean towards the coast at x_i position there will be a discontinuity y_i referring to the variation in wave amplitude is small offshore and larger near the coast, that is, in order of tens of centimeters. Our methodology consist in to use some equidistant or not points $(x_j, y_j),\ j < i$, where the y_j are estimated by the usual equation (25) and after these points are used with the cubic splines for smooth the discontinuities as show the Figure 4. For more details see the book of Howard and Rorres [10] and Cheney and Kincaid [3].

3 Results and Discussions

In Figure 2, a perturbation was created in region D, generating a tsunami that carries this disturbance, that is, it carries energy and only when it gets close to the coast, it carries water with the implication on the height of the wave reaches the coast is due the conservation of energy, acording to Helene and Yamashita [9]. As reported by Ammon *et al*. [1] the most rapid slip occurred in the first $700 - 800\ km$ of the rupture. Bilham [2] said that first $650\ km$ of the rupture appears to be the source zone responsible for the generation of the principal tsunami. In according to Lay *et al*. [11], the source region for strong initial tsunami excitation extends 600 to $800\ km$ north of the epicentre, terminating near the Nicobar Islands. According to the aforementioned authors, the northern third of the aftershock zone appears not to have produced rapid vertical ocean-bottom displacement capable of generating large tsunami waves.

Considering these data, the rapid slips between 10 to $20\,m$ in the extension at $700 - 800\,km$ of the rupture zone and the depth of sea to generate long waves we assumed the model proposed by Gahalaut *apud* Shearer and Burgmann [15] for the finite-slip and in this sense we conjecture the probably local for the origin of the principal tsunami was at $8.45^oN; 93.4^oW$ at approximate $630\ km$ from the epicentre of the principal shock as can be seen in Figure 5.

Figure 5 $-$ (a) Fault slip of up $10 - 15\,m$, in Nicobar segment based in Gahalaut *et al*. [7]
(b) Possible origin local of main tsunami

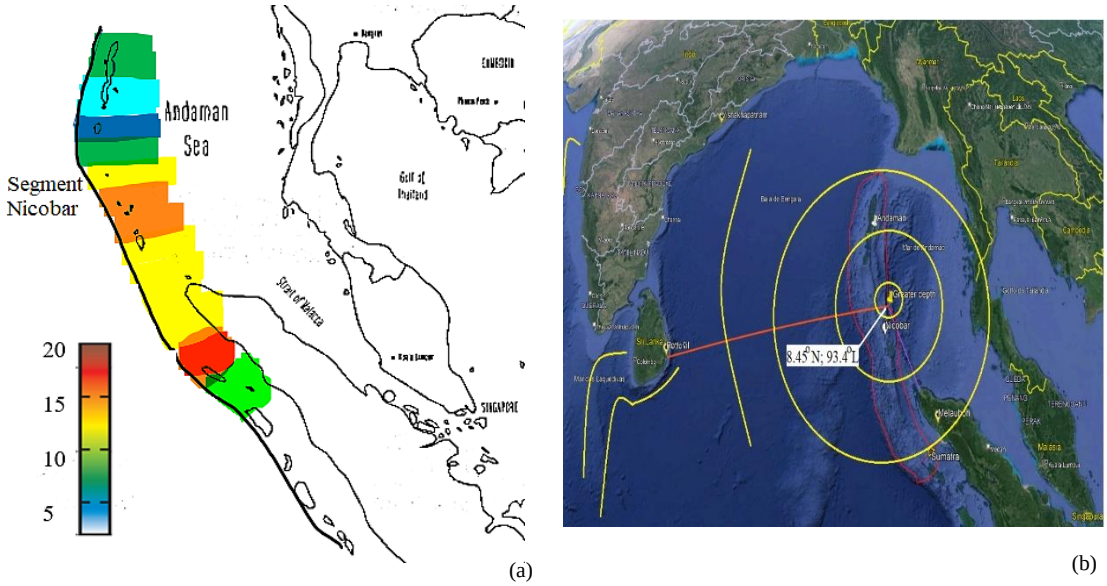

Source: Authors' elaboration.

As reported by Bilham [2], shifts in the sea floor displaced more than of seawater, generating a tsunami that travelled almost all over the planet. This shift was due the brutal vertical deformations (uplift) and subsidence due the slips up to from the Indian Plate under the Burma Plate. The tsunami energy computed for a composite slip model with fast slip ($50\,s$ rise time) in the southern portion of the rupture and slow slip ($3500\,s$ rise time) in the north was estimated by Lay *et al.* [11] firstly as $E_{tsu} = 4.2 \times 10^{15}$ and later revised by $E_{tsu} = 7.8 \times 10^{15}$. The impulse of this mass of water upwards, few minutes after the main shock, it was the force of inertia responsible for disturbing the local system belonging to restoration the force of gravity producing long waves. Considering the different depths of the Indian Ocean in this region until Banda Aceh was used the linear theory of water waves already describes here with the equations (16), (18) and section 2.2 to obtain a pictorial Figure 6 for the motion of the principal tsunami, estimates for its velocity, arrives time in the locality of Banda Aceh and it's energy. The initial amplitude was recorded by tide gauges at $2.17\ m$ as reported by Merrifield *et al.* [13].

Figure 6 – A pictorial form of the tsunami motion in Banda Aceh direction

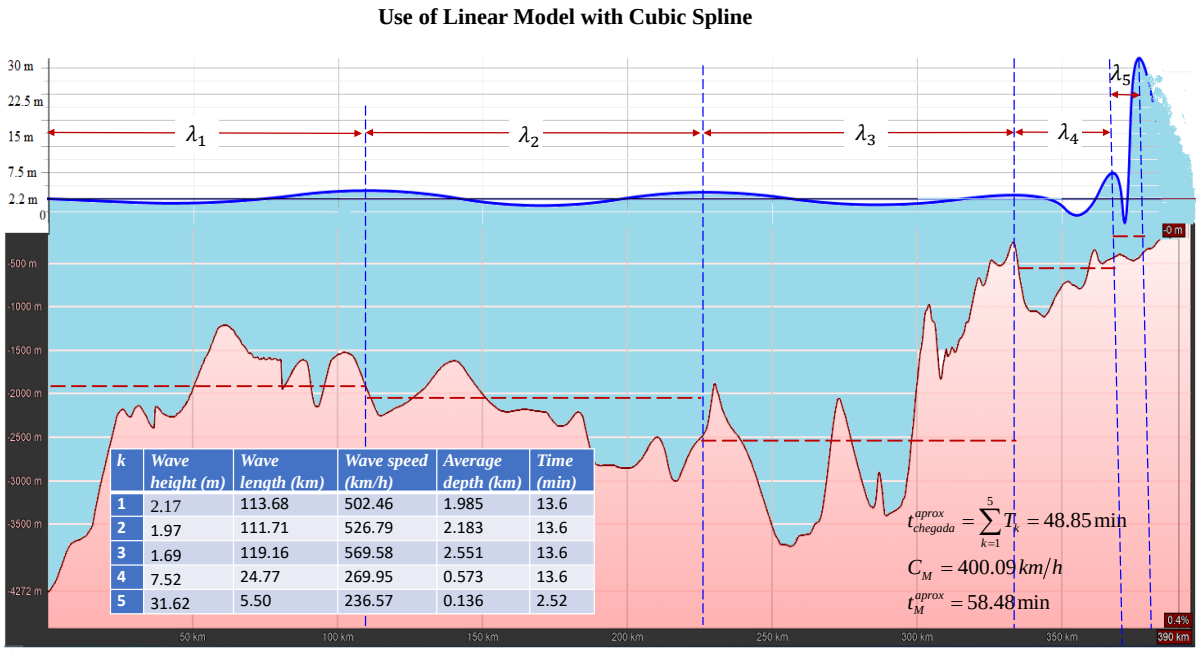

k	Wave height (m)	Wave length (km)	Wave speed (km/h)	Average depth (km)	Time (min)
1	2.17	113.68	502.46	1.985	13.6
2	1.97	111.71	526.79	2.183	13.6
3	1.69	119.16	569.58	2.551	13.6
4	7.52	24.77	269.95	0.573	13.6
5	31.62	5.50	236.57	0.136	2.52

Source: Authors' elaboration. Elevation profile obtained with Google Earth Pro.

In the final of the evolution, *i.e.*, near of the coast d is close of $50\ m$, the linear theory was not more applicable, is not small with respect to wave length. The simple model considered five regions at different constant depth with the last one closest to the coast, *i.e.*, at d is closed $4.5\ km$ distant. In each one was applied the equations (14), (15), (16) and (23) and cubic spline interpolation. Each

constant depth is considered an approximation for the real depth with the minimization of the each area using the Mean Value Theorem for Integrals as showed the Figure 7. Our estimate of arriving at the impact or the tsunami arrival time agreed with the observed time at approximately $57\ min$ in Banda Aceh, as shown in the Figure 6.

The Figure 7 shows seabed elevation profile for the first $120\ km$ of the wave traveling towards the coast of Banda de Aceh from the origin estimated here.

Initially, points (x_i, y_i) were chosen along the first segment in order to portrait the greatest variations in depth. Subsequently, these points were interpolated by a polynomial of degree $n = 3$, as shown in Figure (7b). Then, the area below this polynomial interpolation was calculated and is equal to the area of the rectangle with height k_1 and base λ_1, with k_1 obtained using the mean value theorem for integrals resulting in the segmented dashed line, shown in Figure 7.

The concordance between the values obtained by the interpolated polynomial and the constant k_1, in the first segment, was about 91%. This concordance was determined by the indicator of the quadratic residue, as reported by Young [19]. Similarly, the other constants k_2, k_3, k_4 and k_5 were calculated for the subsequent segments, as shown in Figure 6, with approximate indicators about $R_2 = 78\%, R_3 = 83\%, R_4 = 93\%$ and $R_5 = 94\%$.

Figure 7 – (a) Elevation profile of the ocean floor of the first $120\ km$ traveled
(b) Interpolating polynomial and the red line corresponds to the average value obtained with the Mean Value Theorem for Integrals

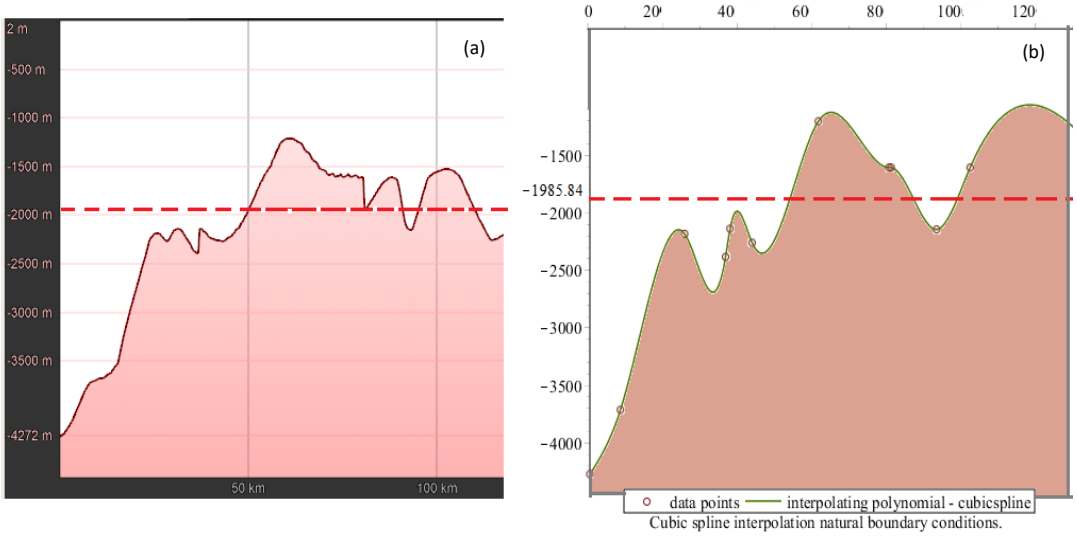

Source: Authors' elaboration.

When the tsunami approached for this coastal region with d approximately $50\ m$, the speed reaches close at $80\ km\ h^{-1}$ and so still very fast and larger to outrun a running person or even using a car. The increase in height as the tsunami reaches the shore of Banda Aceh was reported by Shearer and Burgmann [15] as $10-50\ m$ of amplitude. In our model the amplitude at approximately $4.5\ km$ of shore was estimated in approximate $31\ m$ was based on equation (24). As the period no changes with the depth this implies that the typical time separating the different wave water originated by the tsunami is approximately $13.6\ min$. For the obtaing estimates to energy of the tsunami we defined using equation (19) the 1-D energy of the water wave as

$$\tilde{E}(x,t) = bE_{\lambda}\left(x, z=\eta(x,t), t\right), \quad (J), \tag{26}$$

where b is the extension of the front wave. The Figure 8 was obtained using Maple software, where it shows a probably representation for the tsunami energy in the range $0 \leq x \leq \frac{\lambda_1}{4}$, where λ_1 designates the first wavelength from the origin of the tsunami and its value in km (Figure 6). Hence using the equation (26) and $b = 2\pi\lambda_1$ in the positive x direction and $t = T$, the wave crest is located at $x = 0$ for a time interval equal to the period of the oscillation $T = \frac{2\pi}{\sigma}$. In particular, $\tilde{E}(0, t = T) = bE_{\lambda}(0, a, t = T) = 2.9 \times 10^{15}(J)$.

Figure 8 – The tsunami energy profile: $\tilde{E}(x, t = T)$ is the 1-D energy; $\tilde{E}_p$ is the 1-D potential energy; Dean equation (22), E_{av} is equation (21), E_C is kinetic energy

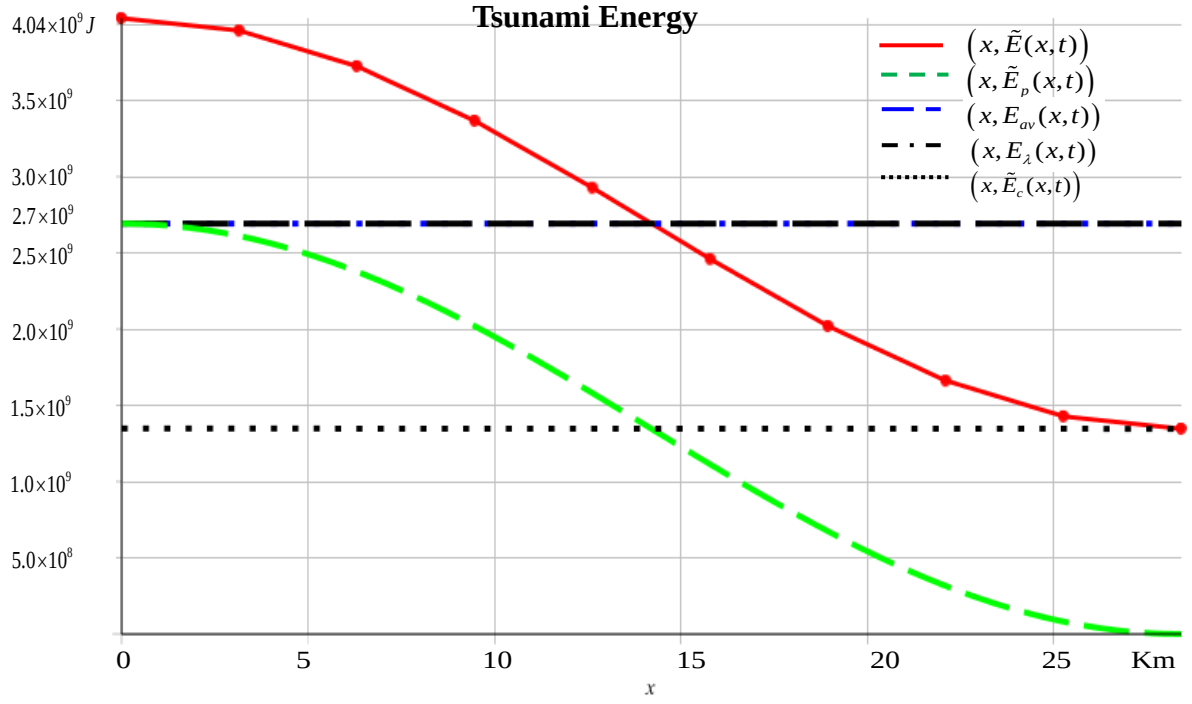

Source: Authors' elaboration.

The $bE_\lambda(0, a = 2.17, t = T) = 3.0 \times 10^{15}(J)$ although shorter than the $E_{tsu} = 7.8 \times 10^{15} J$ reported by Lay *et al.* [11] is significant and equivalent at 55 atomic bombs, once one atomic bomb has $5.25 \times 10^{13}(J)$. As said Shearer and Burgmann [15], unfortunately, there were no gauges near Banda Aceh or in Burma, and a gauge at Port Blair in the Andaman Islands had timing problems. These tide gauge records reported maximum amplitudes of 1 to $3\,m$, typically two to five times smaller than maximum tsunami run-ups from the same areas. Still second these authors, run-up observations depend strongly on near-coastal bathymetry and local site conditions and thus are not ideal for quantitative modelling of tsunamis. As mentioned in the introduction the accuracy in this type of event is difficult. If we assumed of the topographical observations that the extension of the coast of Banda Aceh is about approximate $390\ km$ so can be estimated the energy with the tsunami arrives in this locality, *i.e.*, $E_{tsu}^{B.Aceh}\,(x = 0, z = 2.17, t) = 1.6 \times 10^{14}\ (J)$, that is equivalent at 3 atomic bombs! Helene and Yamashita [9] reported a simple model for understanding the tsunami considering the reflected, transmitted, refracted and diffracted aspects of a tsunami. So theirs model would need of accuracy data of the bathymetry of the ocean and in this sense our model seems easier to be applied. More recently Varsoliwala and Singh [18] developed a numerical solution for a mathematical model of tsunami wave by Elzaki Adomian Decomposition Method where these model is based on shallow-water from the assumption that the vertical component of the acceleration $\dfrac{D\vec{V}}{Dt}$ can be neglected, according to Toro [17], resulting in a not linear theory with more difficult treatment. Unfortunately does not show how these estimates were obtained this value for the tsunami energy.

4 Final Considerations

The model developed here was with based on the classic linear theory of small amplitudes water waves and was showed that it can be used to describe approximately the form of the tsunami profile that arrived in Banda Aceh or possibly too in other regions. The estimate of the tsunami arrival time in Banda Aceh was in reasonable agreement with the real observation time, which seems to indicate the most the probable place of the Tsunami origin near the Banda Aceh coast established in this study. Although the estimates of the tsunami energy were shorter than the reported by the others authors, they were still significant to describe the impact of the event in this region. The use of Cubic Splines interpolation to smooth variations in amplitudes of the main water wave allowed a pictorial representation of these movement in the direction of the Banda Aceh coast.

References

[1] AMMON, C. J.; KANAMORI, H.; LAY, T; VELASTCO, A. A. The 17 July 2006 Java tsunami earthquake. **Geophysical Research Letters**, v. 33, n. 24, p. 1-5, 2006. DOI: https://doi.org/10.1029/2006GL028005.

[2] BILHAM, R. A Flying Start, Then a Slow Slip. **Science**, v. 308, n. 5725, p. 1126-1127, 2005. DOI: https://doi.org/10.1126/science.1113363.

[3] CHENEY, W.; KINCAID, D. **Numerical Mathematics and Computing**. 6. ed. United States: Thomson Brooks/Cole, 2008.

[4] DEAN, R. G.; DALRYMPLE, R. A. **Water Wave Mechanics for Engineers and Scientists**. v. 2. Singapore: World Scientific, 1991.

[5] DEBNATH, L.; BHATTA, D. **Integral Transforms and Their Application**. 3. ed. New York: CRC Press, 2015.

[6] FOX, R. W.; MCDONALD, A. T.; PRITCHARD, P. J.; LEYLEGIAN, J. C. **Introdução à Mecânica dos Fluidos**. 8. ed. São Paulo: LTC, 2010.

[7] GAHALAUT, V. K.; NAGARAJAN, B.; CATHERINE, J. K.; KUMAR, S. Constraints on 2004 Sumatra-Andaman earthquake rupture from GPS measurements in Andaman-Nicobar Islands. **Earth and Planetary Science Letters**, v. 242, n. 3-4, p. 365-374, 2006. DOI: https://doi.org/10.1016/j.epsl.2005.11.051.

[8] GUIDORIZZI, H. L. **Um Curso de Cálculo**. 5. ed. São Paulo: LTC, 2001.

[9] HELENE, O.; YAMASHITA, M. T. Understanding the tsunami with a simple model. **European Journal of Physics**, v. 27, n. 4, p. 855-863, 2006. DOI: https://doi.org/10.1088/0143-0807/27/4/016.

[10] HOWARD, A.; RORRES, C. **Álgebra Linear com Aplicações**. Trad.: Claus Ivo Doering. 10. ed. Porto Alegre: Bookman, 2012.

[11] LAY, T.; KANAMORI, H.; AMMON, C. J.; NETTLES, M.; WARD, S. N.; ASTER, R. C.; BECK, S. L.; BILEK, S. L.; BRUDZINSKI, M. R.; BUTLER, R.; DESHON, H. R.; EKSTRÖM, G.; SATAKE, K.; SIPKIN, S. The Great Sumatra-Andaman Earthquake of 26 December 2004. **Science**, v. 308, n. 5725, p. 1127-1133, 2005. DOI: https://doi.org/10.1126/science.1112250.

[12] MANGARITONDO, G. Explaining the physics of tsunamis to undergraduate and non-physics students. **European Journal of Phisics**, v. 26, p. 401-407, 2005. DOI: http://dx.doi.org/10.1088/0143-0807/26/3/007.

[13] MERRIFIELD, M. A.; FIRING, Y. L.; AARUP, T.; AGRICOLE, W.; BRUNDRIT, G.; CHANG-SENG, D.; FARRE, R.; KILONSKY, B.; KNIGHT, W.; KONG, L.; MAGORI, C.; MANURUNG, P.; MCCREERY, C.; MITCHELL, W.; PILLAY, S.; SCHINDELE, F.; SHILLINGTON, F.; TESTUT, L.; WIJERATNE, E. M. S.; CALDWELL, P.; JARDIN, J.; NAKAHARA, S.; PORTER, F.-Y.;

TURETSKY, N. Tide gauge observations of the Indian Ocean tsunami. **Geophysical Research Letters**, v. 32, p. L09603, 2004. DOI: https://doi.org/10.1029/2005GL022610.

[14] SANTOS, M. L. Tsunami: Que Onda é Essa? **Física na Escola**, v. 6, n. 2, p. 8-11, 2005. Available in: http://www.sbfisica.org.br/fne/Vol6/Num2/a04.pdf. Access at: November 27, 2023.

[15] SHEARER, P.; BURGMANN, R. Lessons Learned from the 2004 Sumatra-Andaman Megathrust Rupture. **Annual Review of Earth and Planetary Sciences**, v. 38, p. 103-131, 2010. DOI: https://doi.org/10.1146/annurev-earth-040809-152537.

[16] STOKER, J. J. **Water Waves**: The Mathematical Theory with Applications. New York: Interscience Publishers, 1957.

[17] TORO, E. F. **Riemann Solvers and Numerical Methods for Fluid Dynamics**: A Practical Introduction. Berlin: Springer, 2009. DOI: http://dx.doi.org/10.1007/b79761.

[18] VARSOLIWALA, Archana C.; SINGH, Twinkle R. Mathematical modeling of tsunami wave propagation at mid ocean and its amplification and run-up on shore. **Journal of Ocean Engineering and Science**, v. 6, n. 4, p. 367-375, 2021. DOI: https://doi.org/10.1016/j.joes.2021.03.003.

[19] YOUNG, R. A. Introduction to the Rietveld Method. *In*: YOUNG, R. A. (ed.). **The Rietveld Method**. New York: International Union of Crystallography, 2002.